Applied Catalysis A: General xxx (2016) xxx–xxx

Contents lists available at ScienceDirect

Applied Catalysis A: General

journal homepage: www.elsevier.com/locate/apcata

Effect of Zn addition on the direct synthesis of hydrogen peroxide over supported palladium catalysts

Suli Wang[a], Kaige Gao[a], Wei Li[a], Jinli Zhang[a,b,*]

[a] School of Chemical Engineering and Technology, Tianjin University, Tianjin 300072, China
[b] Key Laboratory for Green Processing of Chemical Engineering of Xinjiang Bingtuan, School of Chemistry and Chemical Engineering, Shihezi University, Shihezi, Xinjiang, 832000, China

ARTICLE INFO

Article history:
Received 26 May 2016
Received in revised form 8 October 2016
Accepted 23 October 2016
Available online xxx

Keywords:
PdZn catalysts
Direct synthesis of hydrogen peroxide
Geometric change
Electronic effect

ABSTRACT

Alumina-supported Pd-Zn bimetallic catalysts were prepared and evaluated for direct synthesis of hydrogen peroxide. The effect of Zn on the catalytic performance was studied via characterizations by transmission electron microscopy (TEM), temperature-programmed reduction (TPR), X-ray photoelectron energy spectroscopy (XPS), temperature-programmed desorption of H_2/O_2 (H_2-/O_2-TPD), CO chemisorption and diffuse reflectance infrared Fourier transform spectroscopy of CO adsorption (CO-DRIFTS). H_2O_2 productivity of up to 25431 mol kg_{Pd}^{-1} h^{-1} was observed with the optimal bimetallic catalyst 1Pd5Zn, much higher than that over the monometallic catalyst 1Pd (8533 mol kg_{Pd}^{-1} h^{-1}). This increase may be attributed to the geometric change caused by the Zn additive and the electronic interactions between Pd and Zn. The addition of Zn increases the isolated Pd sites (the primary active sites for H_2O_2 formation), which can promote H_2O_2 selectivity. PdZn catalysts show a higher Pd dispersion and incremental Pd^0 content than monometallic Pd owing to electronic interactions between Pd and Zn, which result in increased H_2O_2 productivity. However, a high Pd dispersion and incremental Pd^0 content can increase the H_2O_2 hydrogenation rate, negatively affecting the H_2O_2 selectivity.

1. Introduction

Hydrogen peroxide (H_2O_2) has attracted attention in the fields of environmental protection, chemical synthesis, pharmaceuticals, papermaking and wastewater treatment [1,2]. Currently, H_2O_2 is industrially produced by the anthraquinone process involving the sequential hydrogenation and oxidation of an alkyl anthraquinone precursor, which is a high-cost and energy-intensive multi-step process [3]. Direct synthesis of H_2O_2 using raw materials hydrogen and oxygen is considered a promising green process, because it offers remarkable advantages such as atom economy, low energy consumption, and low operation costs [4,5]. However, it is still a challenge to explore an effective catalyst to implement the green direct synthesis process of H_2O_2 on an industrial scale.

A number of metallic catalysts have been studied, involving Au [6–11], Pt [9,12,13], and Pd [14–21] to improve the catalytic activity and selectivity of H_2O_2 in direct synthesis. Pd has been considered the most promising catalytic metallic component, and the effects of other metallic components on the activity of the Pd catalyst have been extensively investigated [22–34]. Hutchings and co-workers reported a H_2O_2 productivity of 110 mol kg_{cat}^{-1} h^{-1} and a H_2O_2 selectivity of 80% over the bimetallic Pd-Au/C catalyst (2.5 wt% Pd, 2.5 wt% Au) at the reaction temperature of 2 °C, which were much higher than the corresponding values obtained over monometallic 5.0 wt% Pd [22]. When the carbon support was pre-treated by acid, Au-Pd bimetallic catalysts showed no activity for hydrogenation/decomposition side reactions, resulting in a high H_2O_2 selectivity (95%) [23]. Subsequently, Hutchings et al. found that PdSn catalysts treated by an appropriate heat treatment cycle can switch off the sequential hydrogenation and decomposition reactions, thus achieving selectivity of >95% toward H_2O_2 at the reaction temperature of 2 °C [32]. Han et al. reported that the addition of a small amount of Pt into the Pd phase (3.3 wt% Pd, molar ratio Pd/Pt = 16) could significantly enhance H_2O_2 selectivity (from 12% to 60%) and productivity (from 990 mol kg_{Pd}^{-1} h^{-1} to 1770 mol kg_{Pd}^{-1} h^{-1}) [31]. Gu et al. demonstrated that the addition of Ag can improve the performance of Pd catalysts, i.e. over the catalyst PdAg-40 (1 wt% Pd, molar ratio Pd/Ag = 40), the H_2O_2 selectivity was 70.9% and the productivity was 7022 mol kg_{Pd}^{-1} h^{-1} at the reaction temperature of 2 °C [33]. Maity et al. reported that the presence of Ni enhanced the catalytic activity of Pd: the con-

* Corresponding author at: School of Chemical Engineering and Technology, Tianjin University, Tianjin 300072, China.
E-mail address: zhangjinli@tju.edu.cn (J. Zhang).

http://dx.doi.org/10.1016/j.apcata.2016.10.023
0926-860X/

centration of H_2O_2 was 356 mM (49 mol kg_{Pd}^{-1} h^{-1}) in 72 h which was about three times higher (~200% increase) than that of H_2O_2 obtained over pure Pd; the PdNi catalyst was also very stable under harsh acidic conditions [34]. For industrial production, it is essential to explore a low-cost effective catalyst with a high productivity of H_2O_2 and low activity for side reactions.

Recently, Childers et al. demonstrated that PdZn bimetallic catalysts showed high selectivity for propane dehydrogenation to propylene owing to the geometric isolation of active Pd atoms surrounded by the inactive metal Zn [35]. Previous theoretical calculations have indicated that the Pd monomers are favorable for the formation of H_2O_2 by suppressing O—O bond scission [36]. Ouyang et al. studied the direct synthesis of H_2O_2 from H_2 and O_2 as well as the side reactions over Pd-Au/TiO_2 catalysts and found that H_2O_2 productivity increased with a decrease in the Pd/Au ratio, suggesting that the Pd monomer surrounded by Au atoms could be the primary active site for H_2O_2 formation [27]. We herein report on the effect of Zn additives on the catalytic performance of Pd catalyst for the direct synthesis of H_2O_2 from H_2 and O_2. In this study, we prepared a series of bimetallic PdZn catalysts on alumina with different metal loadings, and assessed the catalytic performance for the direct synthesis of H_2O_2 (including the sequential side reactions of hydrogenation and decomposition reactions). The reasons why Zn addition can improve the catalytic activity of Pd catalyst were studied, and the catalysts were characterized by TEM, X-ray diffraction (XRD), TPR, XPS, H_2-/O_2-TPD, CO chemisorption, and CO-DRIFTS.

2. Experimental

2.1. Catalyst preparation

Na_2PdCl_4 (99.95%, Energy Chemical, China) was used as the palladium precursor and $Zn(NO_3)_2{\cdot}6H_2O$ (AR, Tianjin Kemiou Chemical Reagent Co., Ltd.) as the zinc precursor. $NH_3{\cdot}H_2O$ (25 wt.%) was purchased from Tianjin Guangfu Fine Chemical Research Institute. Pseudoboehmite (99%, CNOOC Tianjin Chemical Research & Design Institute) was calcined in air at 600 °C for 4 h to obtain γ-Al_2O_3. γ-Al_2O_3 was used as a support to prepare the bimetallic Pd-Zn samples by the sequential impregnation method with the same nominal Pd loading of 1 wt% but varied Zn loadings (1 wt%, 3 wt%, and 5 wt%). The representative procedure to prepare the bimetallic samples is described below.

First, a zinc precursor solution was prepared by adding $NH_3{\cdot}H_2O$ into an aqueous solution of $Zn(NO_3)_2{\cdot}6H_2O$. For example, 2.275 g of $Zn(NO_3)_2{\cdot}6H_2O$ was dissolved in 45 mL of water, followed by drop-wise addition of $NH_3{\cdot}H_2O$ into the solution with stirring to prepare a uniform solution (named the zinc precursor solution). Then, 10 g of alumina support was added into the zinc precursor solution under vigorous stirring for 1 h followed by incubation at 45 °C for 1 h. The obtained suspension was filtered, washed three times with deionized water, and then calcined in air at 300 °C for 4 h after being desiccated at 120 °C for 12 h. Next, the zinc-loaded sample was impregnated with 50 mL of 0.0188 mol/L Na_2PdCl_4 aqueous solution under stirring for 1 h, followed by incubation at 45 °C for 1 h. Finally, the suspension was filtered, washed, dried, and calcined under the same conditions mentioned above to yield the bimetallic sample.

The samples were denoted in terms of the nominal loading amounts of metallic components. For instance, 1Pd1Zn indicates the sample prepared with a nominal Pd loading of 1 wt% and Zn loading of 1 wt% using Al_2O_3 as the support. As a control, the monometallic Pd catalyst (1 wt% Pd, represented as 1Pd) and the monometallic Zn catalyst (3 wt% Zn, represented as 3Zn) were prepared using the procedure mentioned above.

2.2. Catalytic performance test

2.2.1. Direct synthesis of H_2O_2

Prior to the reaction, the samples were pretreated at 300 °C in 10% H_2/Ar for 4 h. The catalysts were evaluated for the direct synthesis of H_2O_2 in a stainless steel autoclave (internally coated with Teflon) with a nominal volume of 150 mL and a maximum working pressure of 10 MPa. The autoclave was equipped with a magnetic stirrer and provisions were made for measuring the temperature and pressure. Typically, 50 mg catalyst and 20 mL of 0.03 M H_2SO_4/methanol solution were loaded into the reactor. The reactor was purged thrice with N_2 (3 MPa) and then filled with 5% H_2/N_2 and 25% O_2/N_2 to provide the H_2-to-O_2 ratio of 1:2 at the total pressure of 3 MPa. The reaction was performed at 2 °C and the stirring rate of 1000 rpm for 15 min, unless otherwise stated. The H_2O_2 content, $n(H_2O_2)$, was measured by titration with acidic $Ce(SO_4)_2$ solution, while the water content, $n(H_2O)$, was determined by the volumetric Karl Fischer method. The productivity is defined as the moles of H_2O_2 produced per kilogram Pd per hour. H_2 conversion and H_2O_2 selectivity were calculated according to the following equations:

$$H_2 \quad \text{Conversion} = \frac{n(H_2O_2) + n(H_2O)}{n(H_2)} \times 100\% \tag{1}$$

$$H_2O_2 \quad \text{Selectivity} = \frac{n(H_2O_2)}{n(H_2O) + n(H_2O_2)} \times 100\% \tag{2}$$

2.2.2. Hydrogenation and decomposition of H_2O_2

H_2O_2 hydrogenation and decomposition reactions were studied with the initial H_2O_2 concentration of 1.0 wt% and the same reaction conditions mentioned above. Hydrogenation experiments were carried out in an atmosphere of 5% H_2/N_2, while the decomposition experiments were only fed with pure N_2. The H_2O_2 conversion rate is defined as the moles of H_2O_2 consumed per kilogram Pd per hour.

2.3. Catalyst characterization

N_2 adsorption-desorption isotherms were measured on a Micromeritics ASAP 2000 instrument at −196 °C. Inductively coupled plasma-atomic emission spectrometry (ICP-AES) was carried out using an Iris advantage Thermo Jarrel Ash device. XRD patterns were measured from 10° to 90° 2q using a Bruker D8 Advance diffractometer equipped with a Si (Li) solid-state detector (SOL-X) and a sealed tube which provides Cu-Ka radiation. TEM analysis was carried out using a JEOL JEM2100F microscope under an accelerating voltage of 200 kV. XPS was recorded using a Kratos Axis Ultra DLD spectrometer employing a monochromated Al-Ka X-ray source (hn = 1486.6 eV), hybrid (magnetic/electrostatic) optics, a multi-channel plate, and a delay-line detector (DLD). All the binding energies were referenced to the C_{1S} peak at 284.8 eV. TPR experiments were performed with an AutoChem BET TPR/TPD (Quantachrome Instruments AMI-90) connected to a thermal conductivity detector (TCD): a sample of 100 mg was heated from room temperature to 600 °C at a heating rate of 10 °C min^{-1} under a flow of 10% H_2/Ar. H_2- and O_2-TPD experiments were performed with an AutoChem BET TPR/TPD (Quantachrome Instruments AMI-90) connected to a thermal conductivity detector (TCD). Prior to adsorption, the catalyst was reduced in 10% H_2/Ar at 300 °C for 60 min, and then cooled down in pure He. Adsorbents of 10% H_2/Ar and 10% O_2/Ar were introduced into the system at 40 °C for 15 min, respectively. Afterwards, the system was purged with He for 15 min. The temperature was ramped from 40 °C to 500 °C at a rate of 10 °C min^{-1} in He. Metal dispersion was measured by CO chemisorption with an AutoChem BET TPR/TPD (Quantachrome Instruments AMI-90). The catalysts were reduced in H_2/Ar at 300 °C

Please cite this article in press as: S. Wang, et al., Appl. Catal. A: Gen. (2016), http://dx.doi.org/10.1016/j.apcata.2016.10.023

Table 1
Chemical compositions and textural properties of calcined catalysts and bare support.

Sample	Pd (wt%)[a]	Zn (wt%)[a]	S_{BET} ($m^2\ g^{-1}$)[b]	V_p ($cm^3\ g^{-1}$)[b]	D_p (nm)[b]
Al_2O_3	–	–	167.53	0.54	12.84
1Pd	0.84	0	162.43	0.51	12.61
1Pd1Zn	0.84	0.82	160.25	0.50	12.48
1Pd3Zn	0.85	2.34	153.81	0.48	12.41
1Pd5Zn	0.85	2.69	152.64	0.47	12.35
3Zn	0	2.60	155.83	0.50	12.46
5Zn	0	2.70	/	/	/

[a] As determined by ICP.
[b] BET surface area, total pore volume (V_p), and average pore diameter (D_p) were measured from the N_2 adsorption-desorption isotherms.

for 60 min and then flushed for 30 min in He. Thereafter, the catalyst was cooled to 40 °C and CO pulses were injected into the system through 10% CO/He. CO adsorption was assumed to be completed when three successive peaks showed the same peak area. A 1:1 CO/Pd molar ratio was assumed to determine the Pd surface content of the catalysts. CO-DRIFTS spectra were recorded with a Nicolet iS10 spectrometer equipped with a mercury-cadmium-telluride (MCT) detector. Before the adsorption, the sample was reduced in 10% H_2/N_2 at 300 °C for 60 min, and then cooled down in a pure N_2 atmosphere. CO gas was introduced into the system at 30 °C for 15 min. The system was purged with N_2 and spectra were collected at a resolution of 4 cm^{-1}. All infrared data were evaluated in Kubelka-Munk units, which are linearly related to the adsorbent concentration in the spectra. The bridge-to-linear-bound ratios reported here do not take into account the differences in extinction coefficients between the adsorption sites, and therefore, the bridge-to-linear-bound does not represent quantitative coverage, but reflects qualitative differences between catalysts [37].

The N_2 adsorption-desorption, ICP, H_2-TPR, H_2-/O_2-TPD, CO chemisorption and CO-DRIFTS investigations were performed with fresh catalysts and the XRD, TEM and XPS investigations were performed using the reduced catalysts.

3. Results

3.1. Catalyst characterization

3.1.1. Catalyst textural properties and chemical compositions

The N_2 physisorption measurement was carried out to determine the textural properties of the catalysts. As listed in Table 1, the γ-Al_2O_3 support exhibits a mesoporous structure with S_{BET} = 167.53 $m^2\ g^{-1}$, V_p = 0.54 $cm^3\ g^{-1}$, and D_p = 12.84 nm. Both the surface area and the total pore volume of the samples reduced upon loading with the metallic components due to pore blockage caused by the metallic components during catalyst preparation [3].

Table 1 also shows the chemical compositions of the samples measured by ICP. It is indicated that the measured amounts of Pd and Zn are lower than the corresponding nominal values, due to incomplete adsorption of metal ions onto the support. In particular, the measured amount of Zn in the 5Zn sample is 2.70 wt%, much lower than the nominal value of 5 wt%, suggesting that the maximum adsorption capacity of Zn on the support is approximately 2.70 wt%. For sample 1Pd5Zn, the Zn amount is about 2.69 wt%, which is consistent with that of 5Zn.

3.1.2. TEM and CO chemisorption

Fig. 1 displays typical TEM images and particle size distribution histograms of the monometallic Pd and Pd-Zn bimetallic samples. The average particle size of 1Pd is 4.22 nm; the average particle size of the bimetallic samples decreases with the loading amount of Zn, with values of 3.49, 2.56, and 2.39 nm for 1Pd1Zn, 1Pd3Zn, and 1Pd5Zn, respectively. It is suggested that the addition of Zn improves the dispersion of Pd.

Table 2
Surface Pd^0 percent and Pd dispersion of catalysts.

Catalysts	Pd $3d_{3/2}$		Pd $3d_{5/2}$		Pd^0 (%)[a]	Pd Dispersion (%)[b]
	Pd^{2+}	Pd^0	Pd^{2+}	Pd^0		
1Pd	341.7	340.0	336.2	334.7	52.7	16.0
1Pd1Zn	341.7	339.8	336.1	334.5	57.2	22.9
1Pd3Zn	341.7	339.6	336.2	334.3	62.4	27.6
1Pd5Zn	341.5	339.1	335.8	333.8	64.9	31.4

[a] Derived from XPS.
[b] Calculated by CO chemisorption.

Table 2 lists the dispersion of Pd particles calculated from CO chemisorption. The sample 1Pd has a Pd dispersion of 16.0%, and the Pd dispersion increased with increasing the Zn loading amount from 22.9% to 31.4% for the bimetallic samples, confirming that the addition of Zn can promote the dispersion of Pd on the alumina support.

3.1.3. XRD

Fig. 2 shows the XRD patterns of the bare support and the catalysts after reduction treatment. All the catalyst samples present almost the same profile as the γ-Al_2O_3 support with no characteristic peaks corresponding to metallic Pd or Pd-Zn alloy. This is attributed to the small metal particles (less than 4 nm) that are lower than the detection limit of the instrument [38]. Previously, the PdZn alloy was reported to be generated from a PdZn bimetallic sample during the facile reduction process of ZnO which was caused by the spill-over of hydrogen from the Pd metal to ZnO [35,38–43]. However, our XRD patterns do not show the formation of PdZn alloy in the prepared samples.

3.1.4. H_2-TPR

H_2-TPR analysis was performed to investigate the reducibility of the unreduced samples and to identify possible interactions between Pd and Zn. Fig. 3 shows the reduction profiles of the various samples. The TPR profile of the 3Zn sample is completely flat and does not show any peak because the reducibility of Zn is stronger than H_2. The monometallic Pd (1Pd) sample displays two peaks at low temperatures (87.7 °C and 111.8 °C). This is ascribed to either the reduction of PdO species that have different interaction strengths with the support, or the two-step reduction of PdO [44]. Moreover, the monometallic Pd sample also presents a H_2 consumption peak at 341.6 °C, attributed to the reduction of subsurface PdO [33]. For the PdZn bimetallic samples, H_2 consumption peaks ranging from 50 to 200 °C are ascribed to the reduction of PdO and ZnO [41,45]. The reduction peaks of PdZn samples shift to lower temperature and merge into one main peak when the Zn loading is more than 1 wt%, indicating that Zn additives enhance PdO reduction. In addition, the reduction peak of subsurface PdO is not observed due to the smaller metallic particle sizes of PdZn samples. Previously, Nilsson et al. reported that the reduction of ZnO can be facilitated in the presence of Pd and H_2 [46]. Therefore, it is reasonable to conclude that Zn can interact strongly with Pd species in the bimetallic samples to change the reducibility.

3.1.5. XPS

XPS analysis was performed to reveal the electronic interactions between Pd and Zn and the valence state of the surface Pd species for the catalysts. Fig. 4a shows the Pd3d XPS spectra of the catalysts. The peaks near 341.7 and 336.2 eV are attributed to Pd^{2+}, while those at 340.0 and 334.7 eV due to Pd^0 species [47]. The relative content of each palladium species of the catalyst is calculated by curve fitting and listed in Table 2. Fig. 4b shows the Zn$2p_{3/2}$ XPS

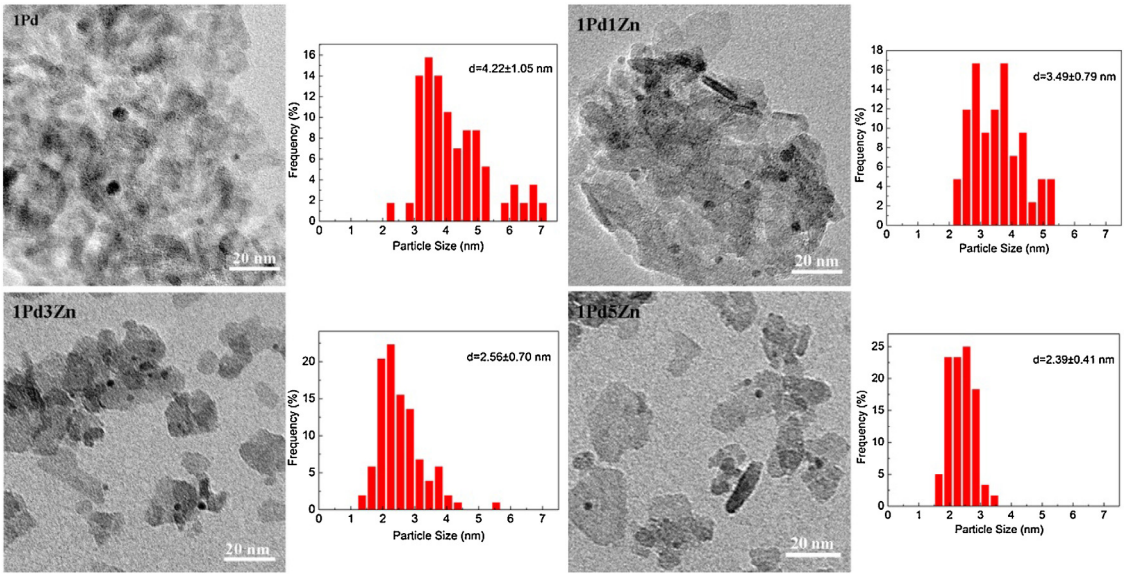

Fig. 1. TEM images of fresh reduced catalysts.

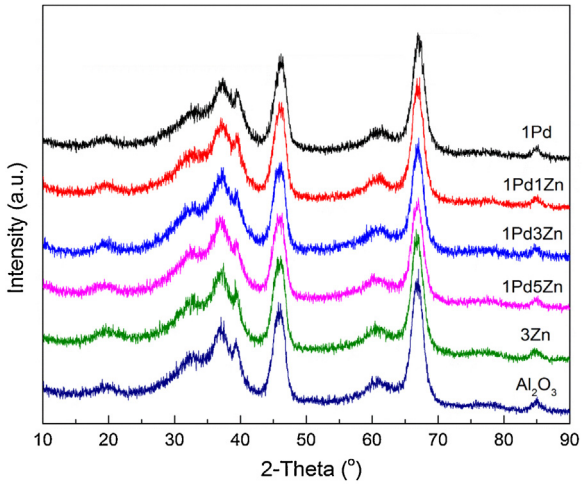

Fig. 2. XRD patterns of the bare support and catalysts after reduction treatment.

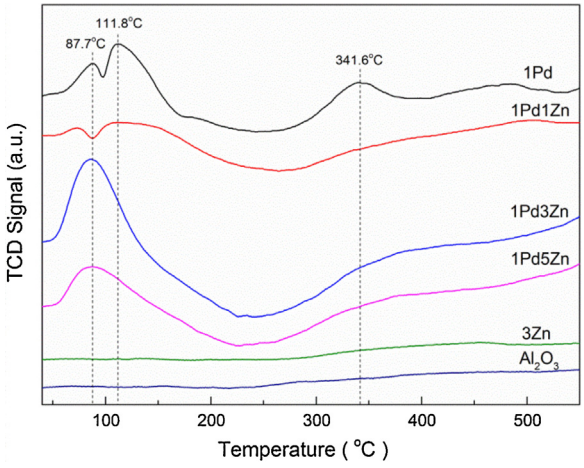

Fig. 3. TPR profiles of catalyst samples.

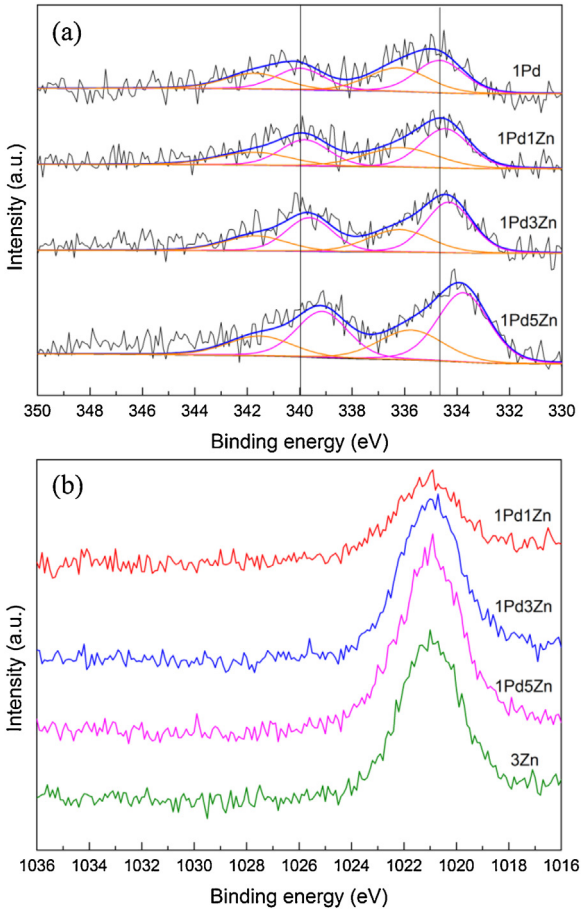

Fig. 4. (a) XPS Pd3d spectroscopy and (b) XPS $Zn2p_{3/2}$ spectroscopy for reduced catalysts.

spectra of the catalysts with the peak around 1021.8 eV due to zinc species [48]. As listed in Table 2, the contents of Pd^0 in the bimetallic samples are higher than that of 1Pd, increasing from 52.7% to 64.9% as the loading of Zn increases from 1 wt% to 5 wt%. It is illustrated that the Zn additives can transfer electrons to palladium species in the bimetallic samples.

Table 3
Desorption amount of H_2 and O_2 and the ratio of bridge-to-linear-bound from DRIFTS over PdZn catalysts.

Sample	Desorption amount of O_2 (mmol g_{Pd}^{-1})	Desorption amount of H_2 (mmol g_{Pd}^{-1})	bridge-to-linear-bond ratio
1Pd	266	3554	7.59
1Pd1Zn	368	4229	6.16
1Pd3Zn	398	4503	5.88
1Pd5Zn	426	4834	3.74

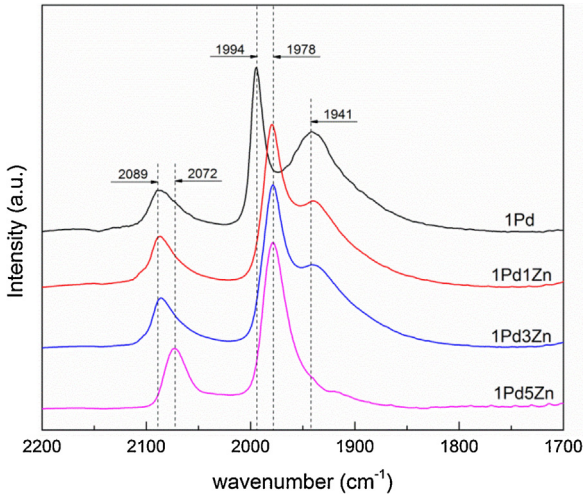

Fig. 5. In situ DRIFTS of CO adsorption over different catalysts.

3.1.6. O_2-TPD and H_2-TPD

The O_2-TPD and H_2-TPD profiles were recorded for all catalysts, as shown in Fig. S1 and Fig. S2 in Supplementary material. Neither the O_2 desorption peak nor the H_2 desorption peak is observed with the 3Zn sample, indicating that the monometallic 3Zn sample lacks affinity towards O_2 and H_2. With the 1Pd sample, the O_2 desorption peak is detected at 216.5 °C, while the bimetallic samples had desorption temperature of 219.5 °C, 277.5 °C, and 233.1 °C for 1Pd1Zn, 1Pd3Zn, and 1Pd5Zn, respectively, i.e. the desorption temperature gradually increases with the loading amount of Zn. In the case of H_2-TPD profiles, a similar tendency is observed, illustrating that the presence of Zn additives enhances the interactions between O_2/H_2 and Pd species. As listed in Table 3, the desorption amounts of both O_2 and H_2 increase strongly with the loading of Zn. Therefore, Zn addition can generate more adsorption sites in the bimetallic catalysts than monometallic 1Pd.

3.1.7. CO-DRIFTS

In situ DRIFTS measurements of CO adsorption were performed to study the nature of the exposed sites of the catalysts. Fig. 5 shows the DRIFT spectra for the monometallic Pd and PdZn bimetallic catalysts. In the case of the monometallic 1Pd catalyst, the bands observed at 2089, 1994, and 1941 cm^{-1} are attributed to CO adsorbed on different metallic Pd sites [49,50]. The peak at 2089 cm^{-1} is related to linear CO species on isolated surface Pd sites [51], 1994 cm^{-1} is assigned to the bridged CO on the Pd edges [52], while 1941 cm^{-1} is due to the bridged CO species on Pd atoms exposed at the surface of either (100) or (111) facets [53]. For the bimetallic catalysts, all three peaks were red shifted; in particular, the peak intensity at 1941 cm^{-1} decreases significantly in 1Pd1Zn and 1Pd3Zn before finally disappearing in 1Pd5Zn. This indicates that the palladium surface structures are significantly modified by Zn. These peaks shifted to lower wavenumber, probably because of the enhanced d-orbital electron density resulting from the charge transfer from Zn to Pd species [27].

Table 4
Performance of all catalysts in H_2O_2 direct synthesis from H_2 and O_2.

Catalysts	Conversion[a] (%)	Selectivity[a] (%)	Productivity[a] (mol kg_{Pd}^{-1} h^{-1})
1Pd	22.9 ± 0.6	64.3 ± 0.4	8533 ± 149
1Pd1Zn	42.8 ± 1.0	76.6 ± 0.4	19000 ± 356
1Pd3Zn	52.4 ± 0.8	77.1 ± 0.2	23125 ± 307
1Pd5Zn	56.6 ± 1.2	78.5 ± 0.5	25431 ± 395
3Zn	0	0	0

[a] Values after "±" represent mean absolute errors.

The bridge-to-linear-bound ratio of the adsorbed CO species was calculated according to individual peak area, as listed in Table 3. This ratio is 7.59 for 1Pd, while it decreased regularly to 3.74 (1Pd5Zn), suggesting that the surface content of contiguous Pd sites is reduced, whereas the number of isolated Pd sites increased as the Zn loading was increased. It has been reported previously that Zn can break up Pd ensembles on the surface, thus reducing the number of neighboring Pd atoms, resulting in the formation of more Pd islands and single Pd surface atoms [35].

3.2. Catalytic behavior

3.2.1. H_2O_2 direct synthesis

All the synthesis experiments were carried out in triplicate to ensure the accuracy of the test. The catalytic performances of all the catalysts are summarized in Table 4. Among the catalysts, the 3Zn sample is not active in the H_2O_2 direct synthesis (the catalytic performance of 1 wt% and 3 wt% Zn behaves similarly), while 1Pd catalyst shows H_2 conversion of 22.9% and H_2O_2 selectivity of 64.3%; the H_2O_2 productivity is 8533 mol kg_{Pd}^{-1} h^{-1}. It is obvious that PdZn bimetallic catalysts show a significant improvement in catalytic performance compared with that shown by the monometallic Pd catalyst. In particular, H_2O_2 productivity increases from 8533 mol kg_{Pd}^{-1} h^{-1} over the 1Pd sample to 25431 mol kg_{Pd}^{-1} h^{-1} over 1Pd5Zn. Simultaneously, Zn addition results in higher H_2O_2 selectivity and H_2 conversion; e.g. 1Pd1Zn has a H_2O_2 selectivity of 76.6% and H_2 conversion of 42.8%. However, increasing the Zn loading cannot increase the H_2O_2 selectivity and the H_2O_2 productivity linearly. The catalytic performance we obtained was comparable to that reported in the related literature (as shown in Table 5).

We also assessed the stability of the catalysts with recycle experiments over 1Pd and 1Pd5Zn. As listed in Table 6, the re-used catalysts exhibited a slight decrease in productivity which resulted from the slight loss of Pd during the direct synthesis process.

3.2.2. H_2O_2 decomposition, hydrogenation and H_2O formation from H_2 and O_2

In order to uncover the possible side reactions over the catalysts, H_2O_2 decomposition and hydrogenation reactions were carried out in H_2O_2-methanol solutions under N_2 and H_2 atmospheres, respectively. For H_2O_2 decomposition reaction, H_2O_2 consumption was not detected over these catalysts (Fig. 6); hence, these catalysts are inert toward the decomposition of H_2O_2 during the reaction. The H_2O_2 hydrogenation rate is 11816 mol kg_{Pd}^{-1} h^{-1} over 1Pd and

Table 5
Catalytic performance of catalysts reported in related literatures.

Reference	Reactor system	Catalyst	Temp (°C)	Pressure (MPa)	Solvent	Selectivity (%)
Chinta [54]	semibatch	5 wt%Pd/SiO_2	10	0.1	H_2O + HCl + Br^-	>90
Chinta [54]	semibatch	5 wt%Pd/SiO_2	10	0.1	H_2O + HCl	60
Edwards [55]	batch	2.5%Au-2.5% Pd/TiO_2	2	4	CH_3OH+ H_2O	95
Edwards [55]	batch	5% Pd/TiO_2	2	4	CH_3OH+ H_2O	22
Ouyang [27]	semibatch	2% Pd-1% Au/TiO_2	10	0.1	C_2H_5OH + H_2SO_4	48.1
Hu [16]	semibatch	2.5%Pd/XC-72	10	0.1	C_2H_5OH + H_2O + HCl	74
Ghedini [56]	batch	2.5%Pd/SBA-15	20	1	CH_3OH+ H_2SO_4	55

Table 6
Stability test of 1Pd and 1Pd5Zn.

sample	Fresh catalyst Pd content (wt%)	Used Catalyst Pd content (wt%)[a]	Pd content in the solution (mg/ml)[a]	Re-use productivity (mol kg_{Pd}^{-1} h^{-1})[b]
1Pd	0.84	0.83	0.49	8169
1Pd5Zn	0.85	0.82	0.87	24800

[a] Catalysts were treated in the working solution under the stirring rate of 1000 rpm at 2 °C and 3 MPa with the atmosphere of 5%H_2/N_2 for 2 h.
[b] Productivity on re-used determined by recovering catalyst after first synthesis, drying in vacuum, and then re-assessing activity under reaction conditions.

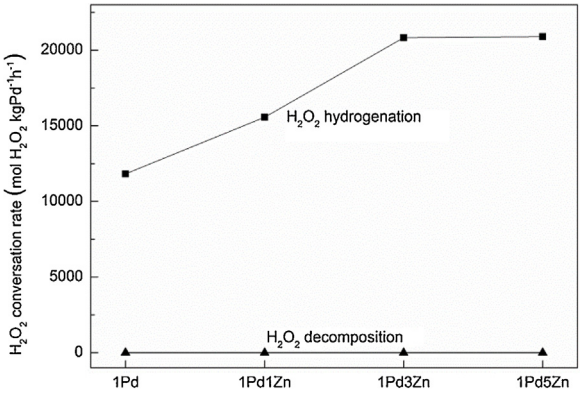

Fig. 6. Decomposition and hydrogenation of H_2O_2 over catalysts.

increases with Zn loading, reaching 20888 mol H_2O_2 kg_{Pd}^{-1} h^{-1} over 1Pd5Zn.

The formation of H_2O from H_2 and O_2 was also examined as a side reaction in this reaction system, which may occur simultaneously during the H_2O_2 synthesis process. We measured the selectivity over the monometallic Pd and PdZn catalysts under low H_2 conversions by shortening the reaction time. At a very low conversion of H_2, the contributions of both the hydrogenation of H_2O_2 and the decomposition of H_2O_2 are negligible to the overall rate of H_2O_2 synthesis [26]. H_2O formation from H_2 and O_2 is the main side reaction responsible for lowering the selectivity of H_2O_2 under such conditions. As shown in Fig. S3 in Supplementary material, the 1Pd catalyst shows a H_2O_2 selectivity of 75.8% at a H_2 conversion of 11.7%, suggesting that the monometallic Pd catalyst is very active in H_2O formation from H_2 and O_2. The H_2O_2 selectivity over the PdZn bimetallic catalysts is higher than 90.0% when the H_2 conversion is approximately 12.0%. Thus, the addition of Zn can effectively inhibit the formation of H_2O from H_2 and O_2.

4. Discussion

Previous studies reported poor activity and selectivity for H_2O_2 by direct synthesis when using Al_2O_3 as a support. For example, Hutchings et al. reported that 5 wt% Pd/Al_2O_3 showed the H_2O_2 productivity of 9 mol kg_{cat}^{-1} h^{-1} with a low selectivity [22]. However, Pashkova et al. obtained different results with respect to the activity and selectivity of Pd/Al_2O_3 [57]. The catalyst (Heraeus K-0219, 5 wt% Pd on Al_2O_3, particle size 10–20 mm) which they used achieved a H_2O_2 selectivity of 82–85% and a productivity of 6500 mol h^{-1} kg_{Pd}^{-1}. Fan et al. demonstrated that both H_2 conversion and H_2O_2 selectivity increased with increasing Pd loading up to a maximum followed by a decrease. H_2O_2 selectivity was about 40% and H_2 conversion was about 60% over the best Pd loading of 1 wt% [58]. The poor catalytic performance of 5 wt% Pd/Al_2O_3 reported by Hutchings is possibly due to the different conditions applied in the direct synthesis process.

The addition of Zn into the Pd catalyst can significantly enhance the H_2O_2 productivity using H_2 and O_2 as the raw materials. From the above experimental results, the function of Zn addition on the H_2O_2 direct synthesis can be explained in terms of the geometric effect and the electronic effect in the bimetallic PdZn catalysts.

In this study, PdZn catalysts show a smaller particle size and higher Pd dispersion than the monometallic Pd sample, as measured by CO chemisorption and TEM. These observations are consistent with the measured catalytic activity, indicating that more exposed Pd atoms on the surface can increase the adsorption capacity of PdZn catalysts towards H_2 and O_2 (as determined by H_2-/O_2-TPD). Therefore a high H_2 conversion and H_2O_2 productivity are achieved over bimetallic PdZn catalysts. In addition, the electronic interactions between Pd and Zn also play a positive role in augmenting the H_2 conversion and the H_2O_2 productivity. As shown by XPS and CO-DRIFTS results, the fraction of Pd^0 increased with the loading of Zn owing to charge transfer between Pd and Zn species. It has been demonstrated that Pd^0 was more active than the corresponding Pd^{2+} in the direct H_2O_2 synthesis [59–63].

From the CO-DRIFTS analysis, the fraction of Pd linearly bound to CO increases at higher Zn loadings, indicating that the Zn additive can promote the formation of more isolated Pd sites and less contiguous Pd ensembles on the surface. It is well known for the direct synthesis of H_2O_2 that the formation of H_2O_2 results from the interaction of atomic H and molecular O_2, while the dissociation of O_2 usually leads to H_2O formation from H_2 and O_2. Therefore, the activation of molecularly adsorbed O_2 without dissociation is pivotal for this reaction system. Theoretical calculations and experimental results have confirmed that isolated Pd surrounded by less active metal atoms are more favorable for H_2O_2 formation than contiguous Pd ensembles by inhibiting O—O bond scission [27,33,36,64]. Therefore, we conclude that the enhanced H_2O_2 selectivity over PdZn bimetallic catalysts is attributed to the isolation of active Pd atoms by the Zn additive.

The addition of Zn results in a higher rate of H_2O_2 hydrogenation over palladium catalysts. The catalytic behavior is related to the high Pd dispersion and the incremental Pd^0 content. First,

PdZn bimetallic catalysts provide more adsorption sites for H_2 than monometallic Pd, which affects the H_2O_2 hydrogenation activity. Secondly, Pd^0 has been demonstrated to have a higher H_2O_2 hydrogenation activity than Pd^{2+} since H_2O_2 has higher propensity to get adsorbed on the Pd^0 sites [59,65].

5. Conclusion

In this work, monometallic Pd and PdZn bimetallic catalysts supported on Al_2O_3 were investigated for the direct synthesis of H_2O_2 from H_2 and O_2. The addition of Zn can significantly improve the catalytic performances of palladium catalysts. The promotional effect of the Zn additive is attributed to both the geometric change and the electronic interaction between Pd and Zn. The addition of Zn was beneficial to increase the dispersity of the active Pd on the Al_2O_3 support surface and also the amount of Pd^0, which result in increased H_2O_2 productivity over the PdZn bimetallic catalysts. The high H_2O_2 selectivity results from the geometric effect between Pd and Zn; the presence of Zn increases the amount of isolated Pd sites and reduces the contiguous Pd sites, effectively suppressing the H_2O formation from H_2 and O_2. However, the incremental Pd^0 content and the increased adsorption capacity of H_2 due to the Zn addition increased the rate of H_2O_2 hydrogenation. Combining the above trends, increasing the Zn loading can result in a weak incremental H_2O_2 selectivity.

Acknowledgements

This work was supported by the National Natural Science Foundation of China (21276179), and the Program for Changjiang Scholars, Innovative Research Team in University (IRT_15R46).

Appendix A. Supplementary data

Supplementary data associated with this article can be found, in the online version, at http://dx.doi.org/10.1016/j.apcata.2016.10.023.

References

[1] J.M. Campos-Martin, G. Blanco-Brieva, J.L. Fierro, W. Ange, Chem. Int. Ed. 45 (2006) 6962–6984.
[2] Y. Han, Z.Y. He, S.L. Wang, W. Li, J.L. Zhang, Catal. Sci. Technol. 5 (2015) 2630–2639.
[3] Y. Han, Z.Y. He, Y.C. Guan, W. Li, J.L. Zhang, Acta Phys. Chim. Sin. 31 (2015) 729–737.
[4] J. García-Serna, T. Moreno, P. Biasi, M.J. Cocero, J.-P. Mikkola, T.O. Salmi, Green Chem. 16 (2014) 2320.
[5] J.K. Edwards, S.J. Freakley, R.J. Lewis, J.C. Pritchard, G.J. Hutchings, Catal. Today 248 (2015) 3–9.
[6] P. Landon, P.J. Collier, A.J. Papworth, C.J. Kiely, G.J. Hutchings, Chem. Commun. (2002) 2058–2059.
[7] M. Okumura, Y. Kitagawa, K. Yamagcuhi, T. Akita, S. Tsubota, M. Haruta, Chem. Lett. 32 (2003) 822–823.
[8] P. Landon, P.J. Collier, A.F. Carley, D. Chadwick, A.J. Papworth, A. Burrows, C.J. Kiely, G.J. Hutchings, Phys. Chem. Chem. Phys. 5 (2003) 1917–1923.
[9] T. Ishihara, Y. Ohura, S. Yoshida, Y. Hata, H. Nishiguchi, Y. Takita, Appl. Catal. A: Gen. 291 (2005) 215–221.
[10] G. Li, J. Edwards, A.F. Carley, G.J. Hutchings, Catal. Today 114 (2006) 369–371.
[11] L. Ouyang, L. Tan, J. Xu, P.-F. Tian, G.-J. Da, X.-J. Yang, D. Chen, F. Tang, Y.-F. Han, Catal. Today 248 (2015) 28–34.
[12] G. Li, J. Edwards, A.F. Carley, G.J. Hutchings, Catal. Commun. 8 (2007) 247–250.
[13] T. Deguchi, H. Yamano, S. Takenouchi, M. Iwamoto, Catal. Sci. Technol. 6 (2016) 4232–4242.
[14] F. Menegazzo, M. Signoretto, G. Frison, F. Pinna, G. Strukul, M. Manzoli, F. Boccuzzi, J. Catal. 290 (2012) 143–150.
[15] J. Kim, Y.-M. Chung, S.-M. Kang, C.-H. Choi, B.-Y. Kim, Y.-T. Kwon, T.J. Kim, S.-H. Oh, C.-S. Lee, ACS Catal. 2 (2012) 1042–1048.
[16] B. Hu, W. Deng, R. Li, Q. Zhang, Y. Wang, F. Delplanque-Janssens, D. Paul, F. Desmedt, P. Miquel, J. Catal. 319 (2014) 15–26.
[17] L. Ouyang, P.-F. Tian, G.-J. Da, X.-C. Xu, C. Ao, T.-Y. Chen, R. Si, J. Xu, Y.-F. Han, J. Catal. 321 (2015) 70–80.
[18] S. Sterchele, P. Biasi, P. Centomo, A. Shchukarev, K. Kordas, A.-R. Rautio, J.-P. Mikkola, T. Salmi, P. Canton, M. Zecca, ChemCatChem 8 (2016) 1564–1574.
[19] N.M. Wilson, D.W. Flaherty, Chem. Soc. 138 (2016) 574–586.
[20] M.-G. Seo, S. Kim, D.-W. Lee, H.E. Jeong, K.-Y. Lee, Appl. Catal. A: Gen. 511 (2016) 87–94.
[21] H.E. Jeong, S. Kim, M.-G. Seo, D.-W. Lee, K.-Y. Lee, J. Mol. Catal. A: Chem. 420 (2016) 88–95.
[22] J.K. Edwards, A.F. Carley, A.A. Herzing, C.J. Kiely, G.J. Hutchings, Faraday Discuss. 138 (2008) 225–239.
[23] J.K. Edwards, B. Solsona, E.N. N, A.F. Carley, A.A. Herzing, C.J. Kiely, G.J. Hutchings, Science 323 (2009) 1037–1041.
[24] J.K. Edwards, J. Pritchard, M. Piccinini, G. Shaw, Q. He, A.F. Carley, C.J. Kiely, G.J. Hutchings, J. Catal. 292 (2012) 227–238.
[25] S.J. Freakley, M. Piccinini, J.K. Edwards, E.N. Ntainjua, J.A. Moulijn, G.J. Hutchings, ACS Catal. 3 (2013) 487–501.
[26] J.K. Edwards, S.J. Freakley, A.F. Carley, C.J. Kiely, G.J. Hutchings, Acc. Chem. Res. 47 (2014) 845–854.
[27] L. Ouyang, G.-J. Da, P.-F. Tian, T.-Y. Chen, G.-D. Liang, J. Xu, Y.-F. Han, J. Catal. 311 (2014) 129–136.
[28] V. Paunovic, V.V. Ordomsky, V.L. Sushkevich, J.C. Schouten, T.A. Nijhuis, ChemCatChem 7 (2015) 1161–1176.
[29] J.K. Edwards, J. Pritchard, L. Lu, M. Piccinini, G. Shaw, A.F. Carley, D.J. Morgan, C.J. Kiely, G.J. Hutchings, w. Ange, Chem. Int. Ed. 53 (2014) 2381–2384.
[30] S. Sterchele, P. Biasi, P. Centomo, S. Campestrini, A. Shchukarev, A.-R. Rautio, J.-P. Mikkola, T. Salmi, M. Zecca, Catal. Today 248 (2015) 40–47.
[31] J. Xu, L. Ouyang, G.-J. Da, Q.-Q. Song, X.-J. Yang, Y.-F. Han, J. Catal. 285 (2012) 74–82.
[32] S.J. Freakley, Q. He, J.H. Harrhy, L. Lu, D.A. Crole, D.J. Morgan, E.N. Ntainjua, J.K. Edwards, A.F. Carley, A.Y. Borisevich, C.J. Kiely, G.J. Hutchings, Science 351 (2016) 965–968.
[33] J. Gu, S. Wang, Z. He, Y. Han, J. Zhang, Catal. Sci. Technol. 6 (2016) 809–817.
[34] S. Maity, M. Eswaramoorthy, J. Mater. Chem. A 4 (2016) 3233–3237.
[35] D.J. Childers, N.M. Schweitzer, S.M.K. Shahari, R.M. Rioux, J.T. Miller, R.J. Meyer, J. Catal. 318 (2014) 75–84.
[36] H.C. Ham, G.S. Hwang, J. Han, S.W. Nam, T.H. Lim, Phys. Chem. C 113 (2009) 12943–12945.
[37] M.A. Vannice, J. Chem. Phys. 75 (1981) 5944.
[38] V.M. Lebarbier, R.A. Dagle, L. Kovarik, J.A. Lizarazo-Adarme, D.L. King, D.R. Palo, Catal. Sci. Technol. 2 (2012) 2116.
[39] A. Karim, T. Conant, A. Datye, J. Catal. 243 (2006) 420–427.
[40] T. Conant, A. Karim, V. Lebarbier, Y. Wang, F. Girgsdies, R. Schlogl, A. Datye, J. Catal. 257 (2008) 64–70.
[41] M. Nilsson, K. Jansson, P. Jozsa, L.J. Pettersson, Appl. Catal. B: Environ. 86 (2009) 18–26.
[42] S. Sterchele, P. Biasi, P. Centomo, P. Canton, S. Campestrini, T. Salmi, M. Zecca, Appl. Catal. A: Gen. 468 (2013) 160–174.
[43] L. Bollmann, J. Ratts, A. Joshi, W. Williams, J. Pazmino, Y. Joshi, J. Miller, A. Kropf, W. Delgass, F. Ribeiro, J. Catal. 257 (2008) 43–54.
[44] B. Ngamsom, Catal. Commun. 5 (2004) 243–248.
[45] N. Iwasa, N. Ogawa, S. Masuda, N. Takezawa, Bull. Chem. Soc. Jpn. 71 (1998) 1451–1455.
[46] M. Nilsson, P. Jozsa, L.J. Pettersson, Appl. Catal. B: Environ. 76 (2007) 42–50.
[47] X. Yang, D. Chen, S. Liao, H. Song, Y. Li, Z. Fu, Y. Su, J. Catal. 291 (2012) 36–43.
[48] M. Lenarda, E. Moretti, L. Storaro, P. Patrono, F. Pinzari, E. Rodriguezcastellon, A. Jimenezlopez, G. Busca, E. Finocchio, T. Montanari, Appl. Catal. A: Gen. 312 (2006) 220–228.
[49] M. Skotak, Z. Karpinski, W. Juszczyk, J. Pielaszek, L. Kepinski, D. Kazachkin, V. Kovalchuk, J. Ditri, J. Catal. 227 (2004) 11–25.
[50] C.W. Yi, K. Luo, T. Wei, D.W. Goodman, J. Phys. Chem. B 109 (2005) 18535–18540.
[51] F. Gao, Y. Wang, D.W. Goodman, J. Phys. Chem. C 113 (2009) 14993–15000.
[52] J.B. Giorgi, T. Schroeder, M. Bäumer, H.-J. Freund, Surf. Sci. 498 (2002) L71–L77.
[53] F. Menegazzo, M. Signoretto, M. Manzoli, F. Boccuzzi, G. Cruciani, F. Pinna, G. Strukul, J. Catal. 268 (2009) 122–130.
[54] S. Chinta, J.H. Lunsford, J. Catal. 225 (2004) 249–255.
[55] J.K. Edwards, E. Ntainjua, A.F. Carley, A.A. Herzing, C.J. Kiely, G.J. Hutchings, Angew. Chem. Int. Ed. 48 (2009) 8512–8515.
[56] E. Ghedini, F. Menegazzo, M. Signoretto, M. Manzoli, F. Pinna, G. Strukul, J. Catal. 273 (2010) 266–273.
[57] A. Pashkova, K. Svajda, R. Dittmeyer, Chem. Eng. J. 139 (2008) 165–171.
[58] S. Fan, J. Yi, L. Wang, Z. Mi, React. Kinet. Catal. Lett. 92 (2007) 175–182.
[59] V.R. Choudhary, C. Samanta, T.V. Choudhary, Appl. Catal. A: Gen. 308 (2006) 128–133.
[60] C. Samanta, V.R. Choudhary, Appl. Catal. A: Gen. 330 (2007) 23–32.
[61] C. Samanta, V.R. Choudhary, Appl. Catal. A: Gen. 326 (2007) 28–36.
[62] C. Samanta, V.R. Choudhary, Chem. Eng. J. 136 (2008) 126–132.
[63] Q. Liu, K.K. Gath, J.C. Bauer, R.E. Schaak, J.H. Lunsford, Catal. Lett. 132 (2009) 342–348.
[64] D.W. Yuan, Z.R. Liu, Y. Xu, Phys. Lett. A 376 (2012) 3432–3438.
[65] C. Samanta, Appl. Catal. A: Gen. 350 (2008) 133–149.